

Carbon nanotubes linked with pitavastatin: synthesis and characterisation

E. Borowiak-Palen · P. Skupin · M. Kruszynska ·
L. Sobotta · J. Mielcarek

Received: 18 October 2009 / Accepted: 17 February 2011 / Published online: 1 March 2011
© Springer Science+Business Media, LLC 2011

Abstract The paper presents a study on functionalisation of multi-walled carbon nanotubes in the area of lattice defects and an attempt to bind the nanotubes with pitavastatin. Carbon nanotubes were synthesised by alcohol-chemical vapour deposition in the presence of the catalyst Fe–Co/MgO. The nanotubes were purified and the product was subjected to chemical functionalisation. Functional groups were introduced in the reaction of the purified nanotubes with thionyl chloride to obtain acidic chlorides linked to pitavastatin. The properties and structure of the nanotubes were analysed by FT-IR and Raman spectroscopies, transmission electron microscopy and liquid chromatography coupled with mass spectrometry. Photochemical stability of pitavastatin linked with carbon nanotubes has been found to be increased.

1 Introduction

Recently, carbon nanotubes (CNTs) have become an alternative carrier transporting particles or molecules of biological activity of therapeutic or diagnostic function into the cells [1–5]. The ever increasing interest in biomedical applications of CNTs follows from their biofunctionality and biocompatibility [6].

A serious drawback of nanotubes is their poor solubility in the majority of solvents, which can be eliminated by

chemical modification. The two most frequently used methods are (i) oxidation with concentrated acids leading to formation of carboxyl groups at the nanotubes ends and at defects and (ii) attachment of various functional groups to the nanotube walls and ends [7–11]. The functionalised nanotubes are capable for permeation through biological membranes, which permits transportation of drug molecules inside the cells and their more effective activity [12, 13]. The new systems of controlled release, including those based on CNTs, permit the use of such substances that could not have been used earlier because of their toxicity or problems with administration.

Recent literature is mostly concerned with the application of carbon nanotubes as carriers of anticancer drugs [14–19]. Wu et al. [20] reported on the use of CNTs modified with amine groups as carriers of bioactive peptides and amphotericin B. The use of CNTs as carriers has improved the activity of immunological system and eliminated the side effects of this antibiotic [21]. Much promising is the application of carbon nanotubes in tissue engineering as a substrate for tissue regeneration [22]. This field has been the subject of interest to Chlopek et al. [23] who performed the cell test with the use of osteoblasts and fibroblasts. They studied the effect of CNTs modified with polysulphone on the lifetime of cells and the amount of collagen produced. The presence of CNTs was found to have a slight weakening effect on the cell viability but resulted in a considerable increase in the amount of collagen produced. This observation was very promising for synthesis of enhanced amounts of collagen which can be applied for regeneration of bones as well as soft tissues and nanotubes can support their development [24].

Experiments indicating the possibility of using CNTs as modern systems transporting drugs into the target cells have prompted studies aimed at checking the toxic effect of

E. Borowiak-Palen
Institute of Chemical and Environment Engineering,
West Pomerania University of Technology, Szczecin, Poland

P. Skupin · M. Kruszynska · L. Sobotta · J. Mielcarek (✉)
Department of Inorganic and Analytical Chemistry,
University of Medical Sciences, Grunwaldzka 6,
60-780 Poznań, Poland
e-mail: jmielcar@ump.edu.pl

this form of carbon on living cells [25, 26]. Results of these studies have proved ambiguous. Pulskamp reports that purified nanotubes are not toxic, but the toxicity comes from amorphous carbon and remains of the catalyst, while Dumortier et al. prove that nanotubes functionalised in the reactions of cycloaddition are not toxic, but the oxidised nanotubes modified with polyethylene glycol [27–29]. According to Magrez et al. [30, 31] the nanotubes are less toxic than graphite and their toxicity appears after functionalisation and generation of carbonyl or carboxyl groups on their surfaces. It is generally assumed that the contrasting results are a consequence of the use in the tests of carbon materials of different purity, containing different functional groups on the surface, different test conditions and different types of cultured cells. The problem is even more complex because the chemical properties of functional groups, even groups of the same type, depend on the size of the nanotube. Therefore, according to many researchers, prior to evaluation of nanotubes toxicity it is very important to establish their physico-chemical properties and the effects of the purification methods applied [32].

The promising results reported from many research centres indicate that the use of carbon nanotubes as drug carriers should increase the efficiency of many drugs and minimise the side effects often accompanying traditional therapy. In our study the model therapeutic substance was pitavastatin (PTV) belonging to the group of statins applied in treatment of hyperlipoproteinemia. PTV is photolabile, it easily undergoes decomposition under illumination, which leads to decreased pharmacological activity and generation of toxic photoproducts [33]. Consequently, its administration can lead to many side effects such as phototoxic, photoallergic and photogenotoxic as the photolabile drugs can undergo decomposition also in the human organism. One of the methods aimed at increasing photochemical stability of therapeutic drugs is based on the use of carrier nanostructures such as liposomes, carbon nanotubes, dendrimers etc. [34, 35].

The aim of this study is to work out a method of attachment of PTV into CNTs, and testing the effect of nanostructure PTV–CNTs on the photostability of PTV.

2 Experimental

2.1 Materials

Multi-walled carbon nanotubes (MWCNT) were synthesised at the laboratory at the Institute of Technology of Inorganic Chemistry and Environment Engineering at the Szczecin University of Technology. MWCNT were obtained by chemical deposition of vapours at 950°C over the catalyst Fe–Co–Mg [36]. PTV (in the form of calcium

salt) was purchased from Cadila Healthcare Ltd., tetrahydrofuran (THF), dimethylformamid (DMF) and thionyl chloride (SOCl_2) were purchased from Sigma-Aldrich, methanol and dioxane were obtained from J. T. Baker and Fluka, respectively. The filters used were PTFE Whatman TE 35, pore size of 0.2 μm , $\varnothing = 47$ mm.

All reagents were of high analytical grade.

2.2 Apparatuses and methods

Vibrational properties of pristine and functionalised nanotubes were analysed by IR absorption with Fourier transform (FT-IR) and Raman spectroscopy. The morphology of the samples have been investigated by means of transmission electron microscopy (TEM). HPLC coupled to mass spectrometer (HPLC–MS) was also employed to characterize the modified MWCNT.

For FT-IR study 200 mg KBr was grounded with carbon nanotubes in 0.01 wt% and then pressed under 10 MPa. The spectra were recorded on a FT-IR spectrophotometer Bruker Vector 22, with the spectral range 4000–500 cm^{-1} , resolution of 4 cm^{-1} and scan number of 32.

Raman spectra were recorded using a Renishaw spectrometer Via Raman, with the laser excitation wavelength of $\lambda = 785$ nm and in the spectral range of 3200–10 cm^{-1} . About 0.05 mg of carbon nanotubes were dispersed in about 20 ml of acetone, deposited in aluminium plates and analysed after air-drying.

2.3 Purification of MWCNT

Purification of MWCNT was carried out in two stages. At first MWCNT was heated in an oven at 300°C in order to remove amorphous carbon. Then the product was introduced into a HCl solution of the concentration of 12 mol/l and subjected to sonication for 1 h to remove the residues of the catalysts. The nanotubes were filtered off on a PTFE filter and washed with deionised water. The washing was continued till getting eluate of pH 6, and then washed with about 50 ml of acetone. The sample was dried for 8 h in a drier at 40°C to obtain purified multi-walled carbon nanotubes *p*-MWCNT.

2.4 Functionalisation of *p*-MWCNT

2.4.1 Preparation of acidic chlorides

A portion of 40.0 mg *p*-MWCNT was placed in a three-necked flask and then 1.6 ml of SOCl_2 and 1.0 ml of DMF were added. The reaction was conducted under reflux at 65°C for 24 h. Then the mixture was filtered through a PTFE filter, washed a few times with THF (~200 ml) in

order to eliminate the unreacted SOCl_2 and other impurities. The product (MWCNT–COCl) was dried for 24 h in a drier at 40°C , then weighted and the mass increase was measured. The mass of the sample MWCNT–COCl was 124.7 mg ($\Delta = 84.7$ mg).

2.4.2 Bonding of pitavastatin

Portions of 10.0 mg each of MWCNT–COCl were placed in two beakers then to one of them 10.0 ml of a 0.005 M (0.021 mg) solution of PTV in THF and to the other 10.0 ml of a 0.005 M solution of PTV in dioxane were added. To each of the samples 1 ml of pyridine was added in order to neutralise the formed HCl and hence to inhibit side reactions. The samples were placed in an ultrasonic bath, and then on a magnetic stirrer. The process was conducted at room temperature preventing the substance from the access of light. The duration of the process depended on the solvent used and was 6 or 4 h for THF and dioxane, respectively. The samples were filtered off through a membrane filter PTFE, washed with THF or dioxane, then with methanol and dried for 24 h in a drier at 40°C . The product of the processes conducted in THF and dioxane was 9.87 and 9.12 mg of functionalised MWCNT–PTV, respectively. The yield of PTV bonding in solutions of THF and dioxane was 98.49 and 91.00%, respectively.

2.5 HPLC–MS analysis

A portion of 3.0 mg of nanotubes functionalised with PTV in THF was placed in a beaker, then 10.0 ml of methanol was added and the mixture was stirred with a magnetic stirrer for 24 h. Afterwards the sample was filtered through a PTFE filter and the filtrate was analysed by HPLC–MS. A liquid chromatograph model 2690 (Waters), equipped with a photodiode detector UV—Photodiode Array (Waters) was used. The substances were separated on a column C-18 Nova-Pak (Waters), of the inner diameter of 3.9 mm and the length of 150 mm. The mobile phase was a mixture acetonitrile:phosphate buffer (pH = 3.5) =45:55 (v/v) flown at the rate of 0.5 ml/min. The pH of the mobile phase was adjusted to pH = 4 by appropriate addition of 10% formic acid. The duration of analysis was 30 min. The mass spectrometer used was model ZQ Waters/Micromass. The spectra were recorded in the range from 100 to 1000 m/z, both in the cationic and anionic forms, using electrospray ionisation (ESI).

2.6 Photodegradation of pitavastatin

Stability of PTV methanol solution (concentration 6.18×10^{-5} mol l^{-1}) was studied. The process was led in

the cylindrical quartz cell ($V = 2.8$ ml). The sample was exposed to the high-pressure UV lamp equipped with a mercuric burner (HBO-200) and emitted radiation in the 300–400 nm range. Maximum of the radiation absorption $\lambda = 365$ nm was obtained as a result of interference and Wood filters selection. After irradiation for a certain time (from 0 to 150 min), the absorbance was made at 319 nm. Time of irradiation was 15 min.

In the same conditions, the PTV eluate obtained according to the procedure described in Sect. 2.5 was irradiated. The photostability testing was monitored at $\lambda = 365$ nm with the use of a physical actinometer. The number of quanta absorbed by the PTV solution was equal 1.84×10^{17} . The energy of irradiation— $E = 1876.60$ [$\text{W} \times \text{h}^{-1} \times \text{m}^{-2}$ —was calculated from the formula given by Mielcarek [37].

3 Results and discussion

3.1 Synthesis and purification of MWCNT

The MWCNT used for our study were obtained in the process of chemical deposition of alcohol-chemical vapour at 950°C over the catalyst of Fe–Co–Mg at the molecular weight ratio of 1:1:60. Each process of carbon nanotubes production, irrespective of the conditions used, leads to generation of some carbon impurities and to the presence of some residues of the catalyst in the final product. For this reason the carbon nanotubes were subjected to the heat treatment at 300°C followed by chemical purification by solving the catalyst residues in chloric acid. The purification step is crucial for the application of carbon nanotubes for medical purposes.

The purification is accompanied by the appearance of lattice defects at which functional groups appear. However, a short time of the purification process did not lead to the significant increase in the number of the defects. According to the alkacymetric titration, the total content of oxygen groups in *p*-MWCNT was 1.2 mmol/g, while the amount of the carboxyl groups was 0.2 mmol/g.

The purified but yet unmodified nanotubes do not show a desired solubility or dispersion ability, which restricts their potential applications. In order to improve these properties the nanotubes were subjected to the functionalisation. From the point of view of biomedical applications functionalisation is necessary for direct or indirect attachment of biologically active molecules. It is also an important measure for reducing the toxicity of MWCNT and improvement of solubility to get a drug carrier of better compatibility.

3.2 Methods of investigation of MWCNT properties and morphology

3.2.1 Transmission electron microscopy (TEM)

Detailed TEM analysis of purified MWCNT was performed. Figure 1 (right panel) presents a typical image of the material, whilst Fig. 1 (left panel) is a close-up of the surface of individual wall of the tube. The bulk sample has the outer diameter ranging from 4 to 25 nm and the number of walls waranking from 3 to 24. The higher resolution microscopic investigation clearly showed well crystallized graphitic structure of the walls. Surprisingly, no amorphous carbon and only residual amount of the catalyst particles were detected in the bulk sample. However, some amorphous species were detected being placed in the interior of the tubes were observe, which could explain rather high intensity of D mode in the Raman spectrum of this sample (presented below—Fig. 2).

3.2.2 Raman spectroscopy

Raman spectroscopy is a powerful technique to study MWCNT via the tangential modes, i.e. the G mode ($\sim 1600\text{ cm}^{-1}$), which is derived from the graphite-like in-plane mode, and the disorder-induced D band ($\sim 1300\text{ cm}^{-1}$). Since the G mode arises from sp^2 C crystalline structures and the D mode from defects and amorphous carbon, the I_G/I_D ratio is commonly used as a measure of the relative sample quality. In the low energy range of Raman response the single and doublewalled carbon nanotubes have additional mode: radial breathing mode (RBM).

All the spectra of the functionalised carbon nanotubes showed the characteristic bands at 1600 and 1300 cm^{-1} (see Fig. 2). The I_G/I_D ratio of *p*-MWCNT is 0.61. The

decrease in the I_G/I_D ratio of PTV functionalised MWCNT indicates an increase in the graphite structure disordering.

3.2.3 Infrared spectroscopy with Fourier transform (FT-IR)

Multi-walled carbon nanotubes modified by introduction of functional groups were subjected to FT-IR spectroscopy.

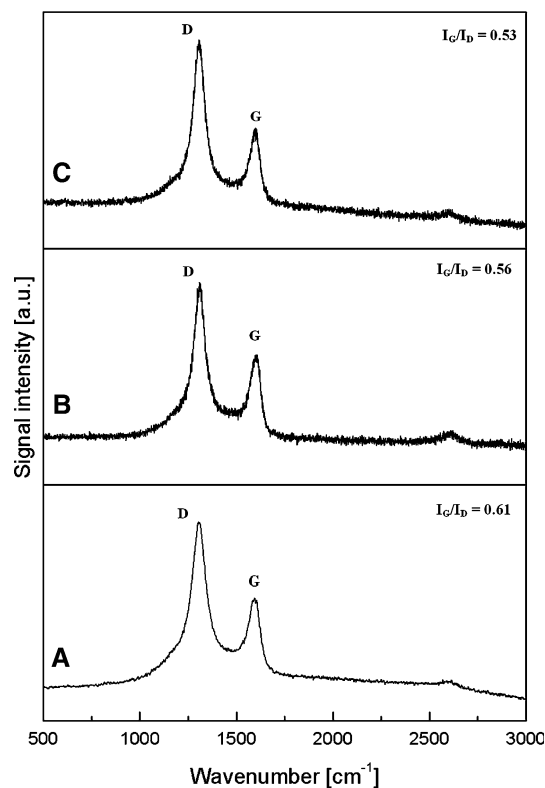
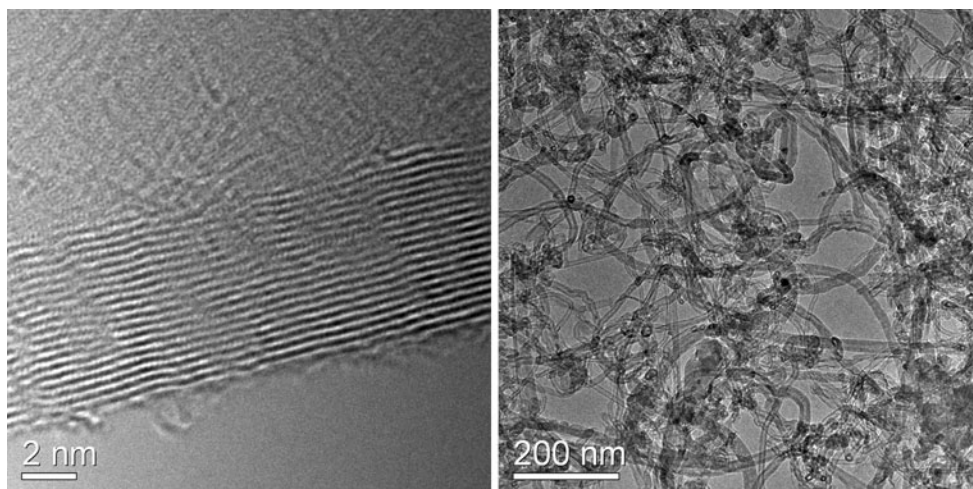


Fig. 2 Raman spectra of *a* purified *p*-MWCNT *b* nanotubes modified with pitavastatin (PTV) in tetrahydrofuran (MWCNT-PTV-THF) *c* nanotubes modified with PTV in dioxane (MWCNT-PTV-dioxane)

Fig. 1 TEM micrographs of purified MWCNT *right panel* a typical image of the material *left panel* a close-up of the wall surface



As shown in Fig. 3a, the spectrum of MWCNT–COCl modified with thionyl chloride has an absorption band with a maximum at 3407 cm^{-1} , proving the presence of stretching vibrations of the O–H bonds and a band with a maximum at $\sim 1384\text{ cm}^{-1}$, characteristic of the bending vibrations of O–H. The band with a maximum at 1702 cm^{-1} , confirms the presence of carbonyl groups (C=O). The weak signal at $\sim 1168\text{ cm}^{-1}$ is assigned to the stretching vibrations of C–O, while the signal at 865 cm^{-1} testifies to the presence of the C–Cl bonds.

For functionalised MWCNT (Fig. 3b) each time a shift of the band related to the stretching vibrations of the carbonyl group was observed. The appearance of weak absorption signals in the range $2300\text{--}2800\text{ cm}^{-1}$, assigned to the stretching vibrations of the C–H bonds, was noted.

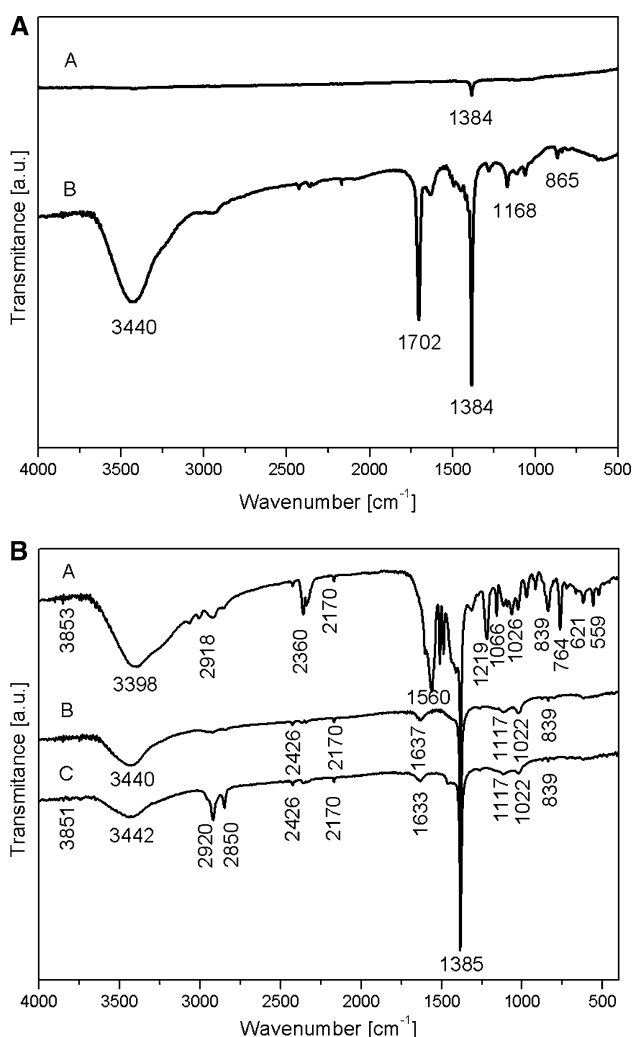


Fig. 3 **a** The FT-IR spectra of: *a* *p*-MWCNT—prior to the reaction with thionyl chloride *b* MWCNT–COCl—after the reaction with thionyl chloride. **b** The FT-IR spectra of: *a* pitavastatin (PTV) *b* MWCNT–PTV complexes obtained in dioxane *c* MWCNT–PTV complexes obtained in tetrahydrofuran

3.3 High performance liquid chromatography–mass spectrometry analysis (HPLC–MS)

Eluate obtained according to the procedure described in Sect. 2.5, was analysed by liquid chromatography coupled with mass spectrometry (HPLC–MS) getting a single peak characterised by the retention time $t_R = 5.68\text{ min}$. The high-resolved mass spectrometry spectrum presented in Fig. 4 displayed a signal assigned to the positively charged molecular ion at $m/z [M + H]^+ = 422.09$ that can be assigned to PTV. No signals that could be assigned to fragmentation ions were observed.

Chromatographic data were supplemented with analysis of electron absorption spectra with photodiode detection. As shown in Fig. 4, the UV spectrum of the substance isolated from the eluate has absorption maxima at $\lambda = 246$ and 319 nm , characteristic of PTV. The above observation is an additional confirmation of the release of PTV during elution of functionalised nanotubes.

It should be emphasised that the use of THF as a solvent resulted in an increase in the yield of the process of PTV bonding to MWCNT–COCl, relative to that obtained for dioxane.

The preparation process of the complexes of functionalised carbon nanotubes with PTV can be schematically shown as in Fig. 5.

3.4 Photochemical testing

The results presented in Sect. 2.6 were applied for quantitative evaluation of photochemical degradation of PTV. Changes in the PTV concentration during irradiation can be described by the following equation according to the first order kinetic reaction:

$$\ln c = \ln c_0 - kt$$

where:

- c* Initial concentration of PTV
- c*₀ Concentration of PTV after certain time of irradiation [mol l^{-1}]
- t* Time [s]
- k* Rate constant [s^{-1}]

On the basis of the equation the rate constants of photodegradation were determined. The calculated rates of photodegradation of free PTV (k_1) and PTV in nanostructure with CNTs (k_2) were $k_1 = 2.7 \times 10^{-4}$ and $k_2 = 8.9 \times 10^{-4}\text{ s}^{-1}$, respectively.

A comparison of the photodegradation rate constants has shown that PTV decomposes three times faster than the nanostructures of PTV–MWCNTs.

Fig. 4 The high-resolved mass spectrometry spectrum and UV spectrum of the product extracted from the MWCNT–PTV (THF) nanostructure

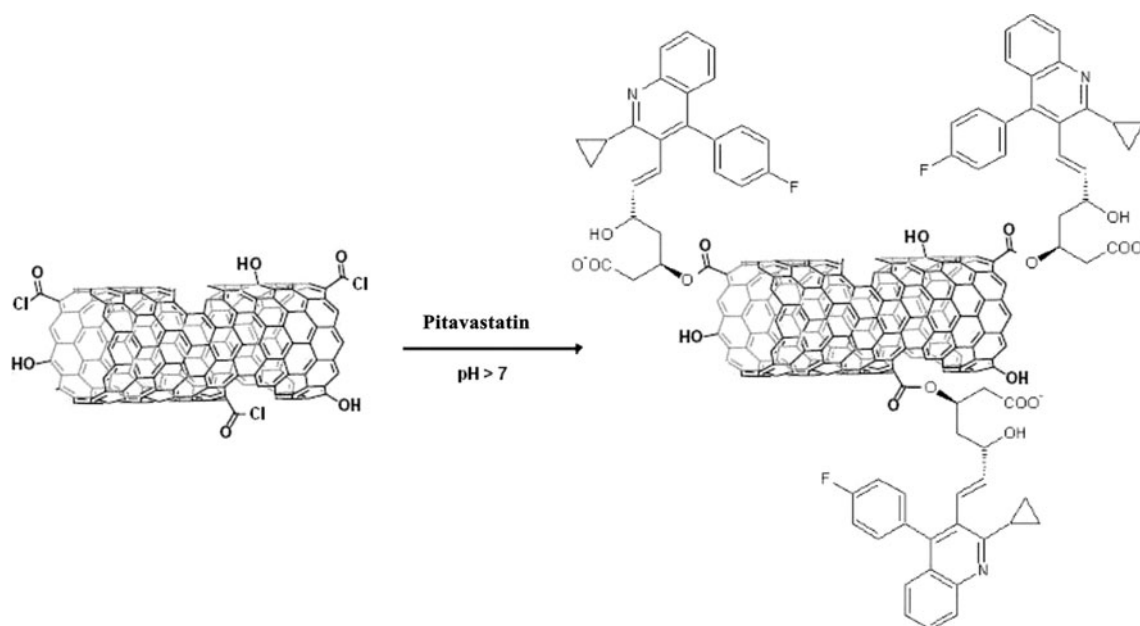
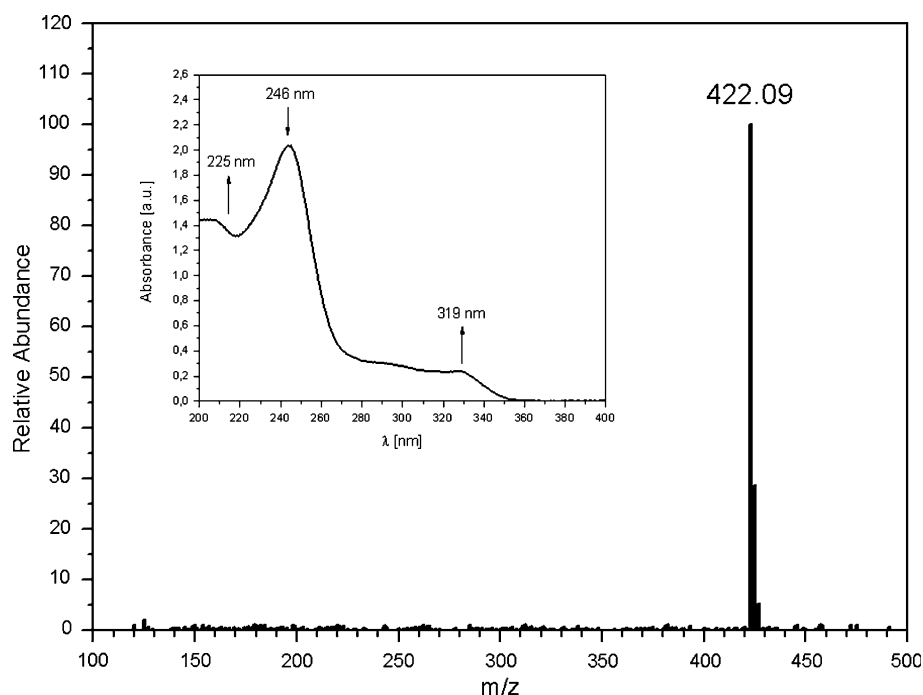


Fig. 5 Schematic presentation of attachment of PTV to functionalised carbon nanotubes

4 Conclusion

Results of the study presented have shown that the method of CNTs functionalisation applied permits obtaining nanostructures with PTV. Importantly, PTV in nanostructures with MWCNTs was found more photochemically stable than in the free form.

References

1. Ilbasmis-Tamer S, Yilmaz S, Banoglu E, Degim IT. *J Biomed Nanotechnol.* 2010;6:20.
2. Wu HC, Chang XL, Liu L, Zhao F, Zhao YL. *J Mater Chem.* 2010;20:1036.
3. Bianco A, Kostarelos K, Prato M. *Curr Opin Chem Biol.* 2005;9:674.
4. Singh S. *J Nanosci Nanotechnol.* 2010;10:7906.

5. Tran PA, Zhang LJ, Webster TJ. *Adv Drug Deliv Rev.* 2009;61:1097.
6. Lobo AO, Antunes EF, Palma MBS. *Mater Sci Eng C.* 2008;28:532.
7. Aitchison TJ, Ginic-Markovic M, Matisons JG, Simon GP, Fredericks PM. *Phys Chem C.* 2007;111:2440.
8. Menard-Moyon C, Venturelli E, Fabbro C, Samori C, da Ros T, Kostarelos K, Prato M, Bianco A. *Expert Opin Drug Discov.* 2010;5:691.
9. Trykowski G, Biniak S, Stobinski L, Lesiak B. *Acta Phys Pol A.* 2010;118:515.
10. You YZ, Hong CY, Pan CY. *Macromol Rapid Commun.* 2006;27:2001.
11. Musso S, Porro S, Vinante M, Vanzetti L, Ploeger R, Giorcelli M, Possetti B, Trotta F, Pederzoli C, Tagliaferro A. *Diam Relat Mater.* 2007;16:1183.
12. Chen X, Schluesener HJ. *Nanotechnology.* 2010;21:105104.
13. Chang R, Violi A. *J Phys Chem B.* 2006;110:5073.
14. Samori C, Ali-Boucetta H, Sainz R, Guo C, Toma FM, Fabbro C, da Ros T, Prato M, Kostarelos K, Bianco A. *Chem Commun.* 2010;46:1494.
15. Pietronave S, Iafisco M, Locarno D, Rimondini L, Prat M. *J Appl Biomater Biom.* 2009;7:77.
16. Ji SR, Liu C, Zhang B, Yang F, Xu J, Long JA, Jin C, Fu DL, Ni QX, Yu XJ. *BBA Rev Cancer.* 2010;1806:29.
17. Bianco A. *MS Med Sci.* 2009;25:125.
18. Bianco A, Kostarelos K, Prato M. *Expert Opin Drug Deliv.* 2008;5:331.
19. Thakare VS, Das M, Jain AK, Patil S, Jain S. *Nanomed UK.* 2010;5:1277.
20. Wu W, Wieckowski S, Pastorin G. *Angew Chem Int Ed.* 2005;44:6358.
21. Shen JD, Huang WS, Wu LP, Hu YZ, Ye MX. *Mater Sci Eng A Struct.* 2007;464:151.
22. Verdejo R, Jell G, Safinia L, Bismarck A, Stevens MM, Shaffer MSP, Biomed J. *Mater Res A.* 2009;88A:65.
23. Chlopek J, Czajkowska B, Szaraniec B, Frackowiak E, Szostak K, Beduin F. *Carbon.* 2006;44:1106.
24. Gould P. *Mater Today.* 2006;9:19.
25. Hussain MA, Kabir MA, Sood AK. *Curr Sci India.* 2009;96:664.
26. Gil PR, Oberdorster G, Elder A. *ACS Nano.* 2010;4:5527.
27. Pulskamp K, Worle-Knirsch JM, Hennrich F. *Carbon.* 2007;45:2241.
28. Gaillard C, Cellot G, Li SP, Dumortier H. *Adv Mater.* 2009;21:2903.
29. Dumortier H, Lacotte S, Pastorin G. *Nano Lett.* 2006;6:1522.
30. Magrez A, Kasas S, V Salicio V. *Nano Lett.* 2006;6:1121.
31. Seo JW, Magrez A, Milas M. *J Phys D Appl Phys.* 2007;40:R109.
32. Maynard AD, Baron PA, Foley M. *J Toxicol Env Heal.* 2004;A67(Suppl 204):87.
33. Grobelny P, Viola G, Vedaldi D, Dall'Acqua F, Gliszczyńska-Swigło A, Mielcarek J. *J Pharm Biomed.* 2009;50:597.
34. Wu AG, Ou P, Zeng LY. *Nano.* 2010;5:245.
35. Raffa V, Vittorio O, Riggio C, Cuschieri A. *Minim Invasive Ther.* 2010;19:127.
36. Costa S, Borowiak-Palen E, Bachmatiuk A, Rummeli MH, Gemming T, Kalenczuk RJ. *Phys Stat Sol.* 2007;244:4315.
37. Mielcarek J, Matłoka A. *Drug Dev Ind Pharm.* 2005;31:861.